water

MDPI

Article

Halosteric Sea Level Changes during the Argo Era

Gongjie Wang [1], Lijing Cheng [2,*], Timothy Boyer [3] and Chongyin Li [1,4]

1 Institute of Meteorology and Oceanography, National University of Defense Technology, Nanjing 210001, China; wanggj_9015@sina.com (G.W.); lcy@lasg.iap.ac.cn (C.L.)
2 International Center for Climate and Environment Sciences, Institute of Atmospheric Physics, Chinese Academy of Sciences, Beijing 100029, China
3 NOAA/United States National Centers for Environmental Information (NCEI), Silver Spring, MD 20910, USA; tim.boyer@noaa.gov
4 State Key Laboratory of Numerical Modeling for Atmospheric Sciences and Geophysical Fluid Dynamics, Institute of Atmospheric Physics, Chinese Academy of Sciences, Beijing 100029, China
* Correspondence: chenglij@mail.iap.ac.cn

Received: 29 April 2017; Accepted: 28 June 2017; Published: 1 July 2017

Abstract: In addition to the sea level (SL) change, or anomaly (SLA), due to ocean thermal expansion, total steric SLA (SSLA, all change to the existing volume of ocean water) is also affected by ocean salinity variation. Less attention, however, has been paid to this halosteric effect, due to the global dominance of thermosteric SLA (TSLA) and the scarcity of salinity measurements. Here, we analyze halosteric SLA (HSLA) since 2005, when Argo data reached near-global ocean coverage, based on several observational products. We find that, on global average, the halosteric component contributes negatively by ~5.8% to SSLA during the 2005–2015 period, and reveals a modest correlation (~0.38) with ENSO on the inter-annual scale. Vertically, the global ocean was saltier in the upper 200-m and fresher within 200 to 600-m since 2005, while the change below 600-m was not significantly different from zero. The upper 200-m changes dominate the HSLA, suggesting the importance of surface fresh water flux forcing; meanwhile, the ocean dynamic might also play a role. The inconsistent pattern of salinity trend between upper 200-m and 200 to 600-m implies the importance of ocean dynamics. Our analysis suggests that local salinity changes cannot be neglected, and can even play a more important role in SSLA than the thermosteric component in some regions, such as the Tropical/North Pacific Ocean, the Southern Ocean, and the North Atlantic Ocean. This study highlights the need to better reconstruct historical salinity datasets, to better monitor the past SSLA changes. Also, it is important to understand the mechanisms (ocean dynamics vs. surface flux) related to regional ocean salinity changes.

Keywords: sea level; halosteric; Argo; thermosteric; salinity; climate change

1. Introduction

The Sea level change, hereafter referred to as sea level anomaly (SLA) to denote change from the long-term mean, is one of the central climate metrics, a measure and consequence of the ongoing global warming. SLA is particularly crucial for the coastal areas that are expected to become more vulnerable to land loss. Therefore, monitoring present SLA, understanding its cause, and projecting future SLA are important topics in climate researches.

Generally, the total SLA can be divided into steric sea level and barystatic sea level components. Total steric sea level anomaly (SSLA) represents all SLA, due to ocean volume increase or decrease (caused by temperature and salinity variations) [1]. Temperature change causes "thermosteric" SLA (TSLA, thermal expansion/contraction of ocean volume), while salinity change leads to "halosteric" SLA (HSLA, saline contraction/expansion of ocean volume). The ocean expands as it warms, which is linked to the thermosteric component of sea level. Seawater density is also a function of salinity: higher

concentration of salt increases the water density and compresses the ocean volume. The halosteric component of SLA is coupled to barystatic SLA, the addition or subtraction of (water) mass to the ocean. To a global approximation over time scales smaller than geologic, the ocean is neither gaining nor losing salt, so any change in globally integrated ocean salinity is linked to addition or subtraction of freshwater.

Many efforts have been made to improve the assessment of historical TSLA and understand its variations [2–7]. However, the salinity-driven HSLA is still poorly understood, and many important scientific questions remain to be fully addressed; e.g.., how much does HSLA contribute to SSLA? What are the mechanisms controlling the salinity changes? This is partly because the effect of salinity on a volume of water is small, compared with the effect of temperature, and has been assumed to be negligible (Warrick et al., 1996). Also, the scarcity of historical salinity observations [8] impede the accurate assessment of past salinity change: Pre-Argo era (before 2005), the salinity measurements mainly came from CTD, Niskin and Nansen (bottle) casts, and amounted to only ~30% of global total temperature observations [9].

Some observational [2,10–13] and reanalysis-based [14] studies have already examined the long term changes of HSLA and highlighted its importance in both regional and global scales. For example, Levitus et al. (2005) analyzed the zonal-averaged HSLA trend during 1955 to 1998, based on the World Ocean Database 2001 (WOD01), and found an opposite trend (compared to the TSLA trend in the Atlantic, a portion of the Pacific (34° N–45° N and 22° S–38° S regions), and the Indian Ocean (a major exception being 28° S–38° S)) [11]. This highlights the rich variability of ocean salinity.

Careful analyses on salinity budgets in the ocean mixed layer have connected the salinity changes with both ocean dynamic process (advection, diffusion etc.) and fresh water flux forcing [15–18]. The long-term ocean salinity change is dominated by the freshwater flux over the sea surface [9,15]. Observational consistency between long-term ocean salinity trends and surface freshwater flux patterns [19,20] provides key evidence for the intensification of the global hydrological cycle [21–23]. On a multi-decadal scale, the halosteric effect contributes to maintaining the thermohaline circulation; hence, its change in the Atlantic Ocean has been long monitored and discussed [2,9,19,20,24,25]. All of these studies suggest that HSLA experienced a non-negligible long-term change. However, rate of long-term HSLA and to what extent it contributes to SSLA is still unclear.

The distribution of salinity in the oceans and adjacent seas varies geographically and with time. Salinity is changed near the sea surface by freshwater flux (evaporation minus precipitation, E-P), salt exclusion associated with sea ice formation, and water input by river runoff [26]. Geographical variations in inputs create regional differences in salinity at the sea surface. Ocean dynamic processes (such as advection, mixing, and diffusion, etc.) carry these differences along, creating large-scale salinity patterns throughout the ocean. On inter-annual scales, ocean salinity is affected by both freshwater flux and ocean circulation variations, which are closely linked to typical interannual variabilities, such as El Niño-Southern Oscillation (ENSO) [14,27,28]. Specifically, Llovel and Lee (2015) highlighted the importance of salinity in positive SSLA in the southeast tropical Indian Ocean during 2005–2013, and provided a hypothetical explanation that an enhanced precipitation in the Maritime Continent region and the observed strengthening of the Indonesian Through Flow (ITF) may account for its origin [29].

Salinity observations have dramatically increased in the recent decade (since 2005), when the Argo data achieved and maintained near-global coverage, dominating the ocean subsurface observations. This provides an opportunity to quantify the contribution of HSLA to the SSLA, by using various independent ocean products for the time period 2005–2015, and also to investigate its regional and vertical changes. This study is organized as follows: Section 2 describes the data and methods used in this study; Section 3 shows the spatial-temporal variability of HSLA, and its role in SSLA during Argo period; Finally, a summary and discussion is given in Section 4.

2. Data and Methods

2.1. Gridded Temperature and Salinity Products

Five different Argo-based temperature (T) and salinity (S) gridded products are used in this study, provided by the following groups: the Japanese Agency for Marine-Earth Science and Technology (JAMSTEC), the Scripps Institution of Oceanography (SCRIPPS), the UK Met Office (EN4), the National Center for Environmental Information (NCEI, the World Ocean Database), and the Institute of Atmospheric Physics (IAP). IAP analysis only provides gridded temperature data currently [30,31], so the salinity analyses shown below are based on the former four products. These data sets are all monthly datasets, with the horizontal resolution of $1^\circ \times 1^\circ$ (from surface layer down to at least 2000-m), and are available for the period of January 2005 to December 2015. In addition, NCEI provides the HSLA estimates since 1955 (from five year running means), so we can compare HSLA during the Argo era with long-term change since 1955, to put the Argo-based analysis into long-term perspective.

The major data source of all these products since 2005 is Argo (SCRIPPS) and the World Ocean Database (EN4, NCEI, JAMSTEC and IAP), including Argo, so a large portion of raw data is the same. The differences among the five analyses reveal the uncertainty in the quality-control processes, mapping methods, and the additional datasets, etc. For example, SCRIPPS analysis only uses Argo profiles to fill the data gaps, while EN4 and NCEI analyses use CTD, bottle, and other in-situ observations, in addition to Argo data. The NCEI uses an objective analysis technique, modified from meteorological use [32], and the other four datasets are based on the Optimal Interpolation method.

2.2. Methods

SSLA, HSLA, and TSLA are calculated by integrating the temperature and salinity anomaly between a definitive layer using the following equations [33]:

$$SSLA = \int_{h_1}^{h_2} (\alpha T' - \beta S') dz \quad (1)$$

$$TSLA = \int_{h_1}^{h_2} \alpha T' dz \quad (2)$$

$$HSLA = \int_{h_1}^{h_2} -\beta S' dz \quad (3)$$

where α and β are the thermal expansion and saline contraction coefficient respectively, calculated from monthly temperature and salinity (following the method in (McDougall, 1987 [34])). Parameter h_1 and h_2 define the lower and upper limits of the layer depth, and the largest value for h_1 is set as 2000-m, which is the maximum depth of SCRIPPS, IAP, and JAMSTEC analyses. For some datasets, pressure instead of depth is available, so we always convert the pressure values to depth before we start our analyses. A 12-month climatology is constructed by averaging the monthly mean values (temperature and salinity, separately) during 2005 to 2015 (in each individual dataset and at each depth in each grid box). Then, the anomaly field is obtained by removing the monthly climatology from each dataset, so a 2005–2015 baseline and the seasonal cycle are removed before our analysis.

The long-term trend is calculated by least square fitting after removing the impact of interannual variability, since it can significantly affect the long-term trend assessment in SLA [35]. Twice the standard error is used here, to represent the uncertainty of the linear trend [36]. The interannual signal (ENSO-related but not exclusive) is derived from a band-pass filter (between 1 to 5 years), based on Fourier analysis. This filter method is based on the assumption that the original time series (for example, global mean HSLA, 132 months) can be linearly decomposed into a series of sinusoidal signals with periods ranging from 2 to 60-month.

3. Results

In this section, we will give a detailed analysis of the spatial and temporal variability of HSLA during the Argo global period (2005–2015), and revisit the role of salinity in SSLA changes.

3.1. Time Evaluation of Global HSLA

Near-global (0° E–360° E, 60.5° S–64.5° N) mean SSLA, TSLA, and HSLA, for the five different products, are shown in Figure 1. Although there are some discrepancies concerning month-to-month variation among different datasets, the SSLA estimates show a positive long-term trend and consistent inter-annual variation since 2005. The trend of SSLA is within 2005–2015 ranges from 0.83 to 0.97 mm/yr for different products (Table 1), with an ensemble mean of 0.86 ± 0.18 mm/yr. This indicates that the long-term rise of steric sea level is detectable by Argo data. The TSLA increase is stronger than the SSLA since 2005 (ranging from 0.81 to 1.01 mm/yr, with ensemble mean of 0.89 ± 0.19 mm/yr), and plays a dominate role in the long-term SSLA changes.

Table 1. The linear trend and associated standard error of steric sea level during 2005–2015, unit: mm/yr. Values are an ensemble mean of all datasets and the two-time standard error.

Trend	SSLA	TSLA	HSLA
SCRIPPS	0.86 ± 0.13	0.88 ± 0.14	−0.02 ± 0.01
JAMSTEC	0.83 ± 0.10	1.01 ± 0.12	−0.18 ± 0.02
EN4	0.97 ± 0.10	0.96 ± 0.12	0.01 ± 0.04
NCEI	0.84 ± 0.17	0.89 ± 0.19	−0.05 ± 0.03
IAP	-	0.81 ± 0.08	-
Mean	0.86 ± 0.18	0.89 ± 0.19	−0.05 ± 0.03
NCEI (1955–2016)	0.63 ± 0.02	0.58 ± 0.02	0.06 ± 0.01

Different from TSLA, HSLA contributes negatively to SSLA on a global scale, with a mean trend of −0.05 ± 0.03 mm/yr, indicating that the global ocean among 60° S–64° N has gotten saltier in the recent decade. Along with anthropogenic global warming, ocean mass has been steadily increasing since 2003 [7], which has had the effect of diluting ocean water. For example, Llovel et al. show that the melting ice and glaciers contribute to about ~70% of the total sea level rise [7]. So, we have a conundrum: the global ocean is being diluted by the addition of freshwater, but our calculations show the ocean is getting saltier. We suggest some possible reasons: (i) it is possible that the associated ocean mass gain mainly affects the high latitude ocean regions, and needs more than one decade to be transported to the mid-latitude and tropical oceans. Therefore, on a global scale, other mechanisms might be the main contributors to the recent ocean saltier trend; (ii) decadal trends in fresh water flux from evaporation, minus precipitation, are larger than the addition of fresh water from melting ice [15]. Both atmospheric reanalysis and satellite-based products reveal a positive global mean freshwater flux (evaporation minus precipitation), which contributes to a saltier ocean [37]; (iii) the relatively short time period, over which the trend is estimated above, may be dominated by the interannual signal obscuring the long-term trend; and (iv) the deep ocean below 2000-m could be a serious candidate to explain the difference [38,39], and calls for more detailed research.

HSLA decreases accounts negatively for about 5.8% of SSLA (ranges from 0 to 22% for different products), and partially offsets the strong thermal expansion (ranges from 0 to 18% and 5.6% for mean percentage of halosteric to thermosteric). This highlights that the halosteric effect can't be neglected on global average. However, HSLA analysis shows larger discrepancies among different datasets than TSLA, due to a smaller signal-to-noise ratio for HSLA than TSLA.

Particularly, estimates of SSLA from SCRIPPS and EN4 include more short-term variability than the other datasets. For example, SCRIPPS TSLA and HSLA are clear outliers for the 2005–2006 period, showing larger month-to-month variation (Figure 1B). EN4 data shows a 2–4 mm larger HSLA decrease in 2005 than the other products, which is probably spurious (Figure 1C). In the following analysis,

we use the ensemble mean of the estimates to show ensemble mean temporal variability (thick black lines in each panel of Figure 1). It is likely that the difference in raw data and mapping methods are responsible for the uncertainty among these datasets.

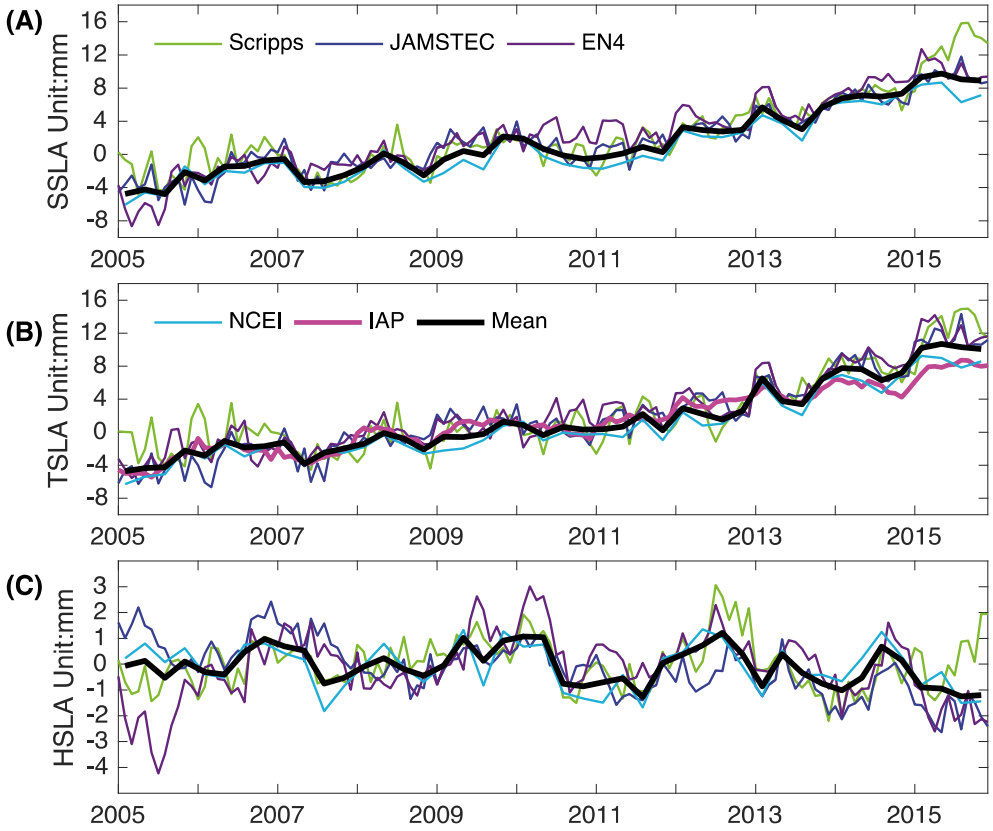

Figure 1. Monthly time series of SSLA (**A**), TSLA (**B**), and HSLA (**C**). Curves show estimates based on products from SCRIPPS, JAMSTEC, EN4, IAP, NCEI, and the mean of the five datasets (black line).

Now, it is worthwhile documenting the HSLA variation since 2005, in the context of a long-time perspective. Figure 2A provides the HSLA from NCEI since 1955, showing a weak positive long-term trend (0.63 $\pm$ 0.02 mm/yr) since 1955, and significant decadal variability (Figure 2A). The HSLA decrease detected by Argo data starts from the early 1990s, so it is possible the Argo data may just be showing one part of a longer cycle. A significant decadal variation of freshwater content has been found in the North Atlantic Ocean, according to a previous analysis [40]. On the other hand, we note that the salinity observations are very sparse pre- this century, so we should be careful to interpret the global salinity change pre-Argo era.

Besides being a robust long-term trend, HSLA shows significant inter-annual variability, which is correlated with ENSO (Figure 2B). The relation between SSLA, along with its thermal component and ENSO, has been comprehensively analyzed by previous studies (i.e., Lombard et al., 2005 [4]). As the fresh water cycle is closely connected with ENSO [27,41,42], HSLA will also be affected. Figure 2B compares the HSLA with an ENSO index—Oceanic Niño Index (ONI), which is calculated as the 3 month running mean of ERSST.v4 SST anomalies in the Niño 3.4 region (5° N–5° S, 120° W–170° W), showing a modest positive correlation (~0.38, exceeding 99% statistical confidence tested with the Student's t-statistic), and confirming the linkage between ENSO and HSLA on an interannual scale. El Niño events bring more precipitation over the global ocean, which results in salinity decrease and an HSLA increase, and vice versa for La Niña events [27].

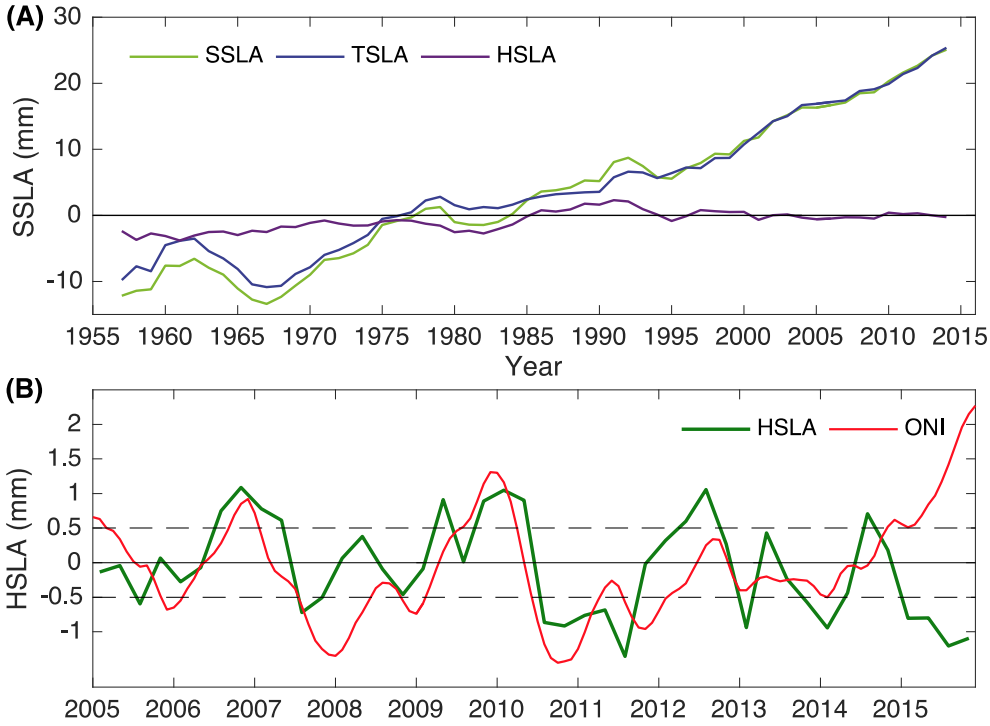

Figure 2. (**A**) SSLA, TSLA, and HSLA, calculated from the NCEI dataset, since 1955; (**B**) The global HSLA time series (ensemble mean of multi-datasets), compared with the Oceanic Niño Index (ONI), since 2005. ONI is available at https://www.esrl.noaa.gov/psd/data/climateindices/list/. 12-month running mean is used to remove the annual cycle.

3.2. Spatial Pattern of Long-Term HSLA Change

The change of HSLA shows rich regional variability, with maximum local trend ~10 times larger than the global mean (Figure 3A). A large-scale HSLA decrease (due to increased salinity) is evident in the subtropical Pacific Ocean (5° N–20° N, 10° S–30° S), the North Indian Ocean (10° S–20° N), and the subtropical Atlantic Ocean (~20° N and ~20° S), in contrast to an HSLA increase (due to decreased salinity) in the Tropical/North Pacific (10° S–5° N, 30° N–60° N), South Indian (30° S–10° S), and Northeast Atlantic Oceans (20° N–60° N). This geographical pattern resembles that of Llovel and Lee (2015) [29], and Durack et al. (2014) [9].

The trend pattern of HSLA, shown above, represents the depth-integrated effect from the surface to 2000-m, so it is worthy investigating the relative contribution from each independent depth. Figure 3B provides the linear trends of the negative product of salinity anomaly and salty contraction coefficient for the four ocean products, from the surface to 2000-m depth. A similar vertical variability is revealed by all datasets in the upper 600-m layer: the upper 200-m layer experiences a slight HSLA decrease (salinity increase), accompanied by a marked HSLA increase (salinity decrease) within the 200-m to 600-m layer. The robust salinity trends are mainly confined to the upper 600-m layer, and below 600-m the contribution to total HSLA is close to zero (−0.03 mm/yr), with an uncertainty of 0.06 mm/yr. It is possible that the large uncertainty below 600-m depth arises from the data source.

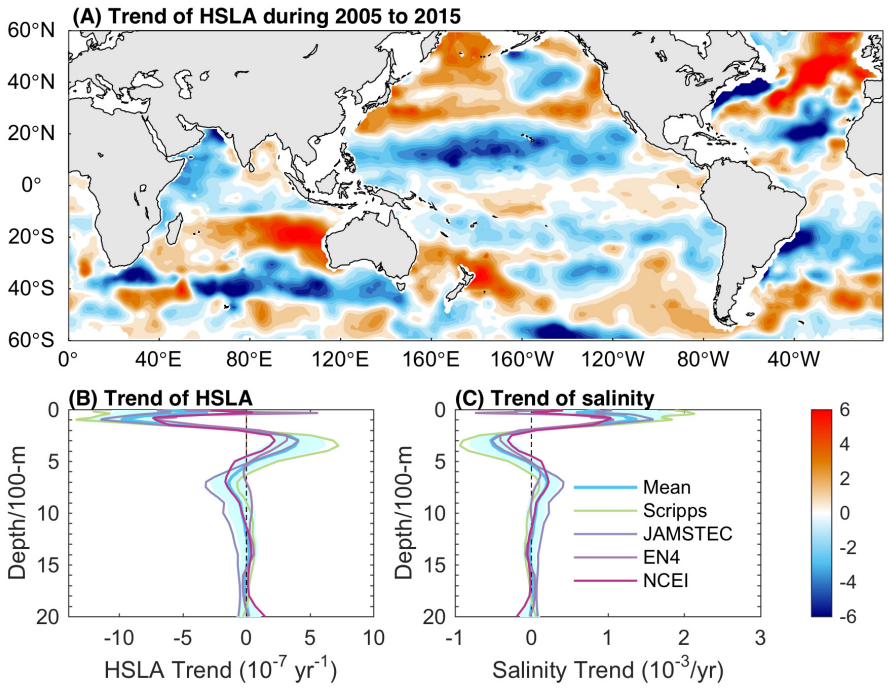

Figure 3. Trend of HSLA over 2005–2015 based on the ensemble mean of all the datasets. (**A**) Geographically pattern, unit: mm/yr; (**B**) Vertically trend in global mean perspective with standard deviation patched; (**C**) the same as (**B**), but with salinity instead.

It is interesting that the globally averaged upper 200-m salinity change is opposite to the change below 200 to 600-m. To explore further, we provide the spatial pattern of the HSLA trend within three different layers: upper 200-m, 200-m to 600-m, and 600-m to 2000-m (Figure 4). The upper 200-m HSLA change largely resembles the mean E-P pattern (i.e., shown in [9,29]), suggesting that surface fresh water flux forcing dominates the large-scale salinity trend [43]. However, within 200 to 600-m, a broad ocean freshening is observed in the Northwest Pacific and Southern Indian Ocean, indicating a different pattern from the upper 200-m. In the Atlantic Ocean and Southern Ocean, upper 200-m and 200 to 600-m of ocean show a similar pattern, probably linked to the meridional overturning current, which brings more vertical mixing of salinity. This highlights the role of ocean dynamics in regulating the ocean salinity changes, in additional to surface freshwater flux forcing. Previous study has suggested the dominance of NAO in the steric sea level change in the North Atlantic: when NAO is positive, the westerlies are shifted northward relative to their mean position, which affect North Atlantic circulation and the transport increases [44]. So potentially, NAO could be one of the plausible reasons for the halosteric change. The Atlantic Ocean below 200-m depth contains comparable magnitude of trend, which indicates that the salinity variability in subsurface layers cannot be neglected. According to Curry et al. (1998) [45], the surface water in the subpolar gyre of the North Atlantic takes 15 or more years to reach deeper depths further south. So, basically, deeper depths are seeing surface conditions from previous years (so it is likely that in the northeast Atlantic, surface conditions 15 years ago were similar to what they are now, only more intense, resulting in the given pattern at deeper depths [40]).

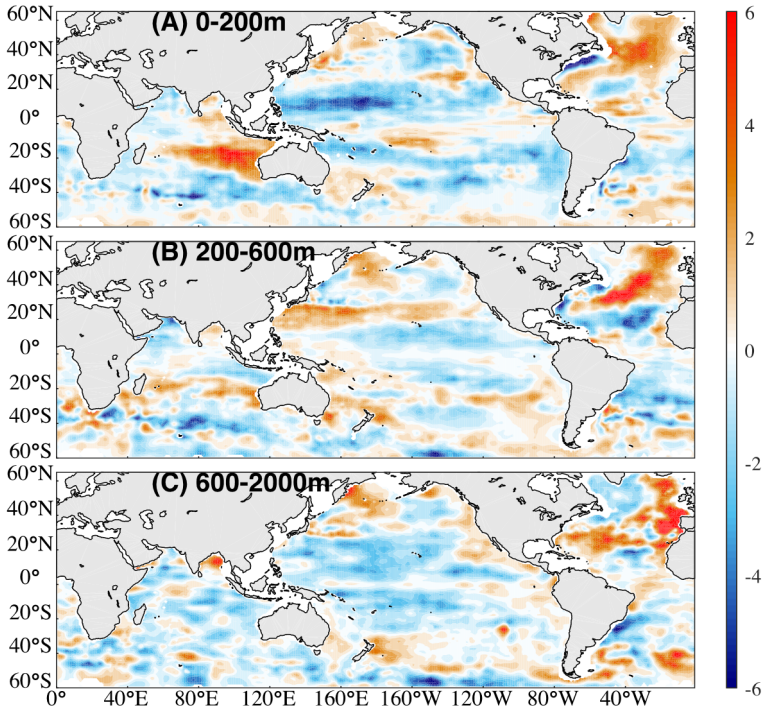

Figure 4. The spatial pattern of HSLA trend (Unit: mm/yr) in the upper 200-m layer (**A**); the 200 to 600-m layer (**B**); and the 600 to 2000-m layer (**C**), between 2005 and 2015. This is the ensemble mean of the SCRIPPS, JAMSTEC, EN4, and NCEI.

The pattern of HSLA change in the upper 200-m layer resembles that of HSLA in the entire upper 2000-m, suggesting the dominant role of upper ocean salinity changes in the total HSLA. This has some importance implications: (1) before the Argo era, there were more salinity observations in the upper ocean than in the deeper ocean. Therefore, if the upper ocean salinity change can be more robustly estimated, we can have a reliable assessment of historical HSLA. This highlights the possibility of accurately re-assessing historical HSLA; (2) nowadays, we still have more observations in the upper layer, since sea surface salinity can be observed from satellites (such as the Soil Moisture Ocean Salinity (SMOS) mission by the European Space Agency and the NASA Aquarius mission). Assimilating the upper ocean surface salinity into ocean models will have the potential to significantly improve the model simulation [46,47].

3.3. The Role of Salinity in Regional SSLA

We have shown in the previous sections that the HSLA contributes negatively to SSLA on global scales, what about the regional changes? Figure 5 shows the zonal mean trend of SSLA for the upper 2000-m (from 2005 to 2015, for the global ocean (A), and three main ocean basins (B–D respectively)). In the Southern Hemisphere, the SSLA is almost completely dominated by the thermosteric component. This is consistent with the observational findings that the Southern Hemisphere experienced its strongest warming in the recent decade, and dominated the global ocean heat content change [48]. Recent publications highlight the intensification of Ekman pumping (associated with changes in wind stress curl), which deepens the isopycnal surface and results in more heat sequestration under the upper ocean layer [49,50]. In the North tropics/subtropics (Equator to 20° N), SSLA is dominated by HSLA, since the mean TSLA changes in this region are around zero over 2005–2015. The North tropical/subtropical Pacific shows opposite changes from the Indian Ocean, due to the strengthening of the Indonesian throughflow, caused by rainfall intensification in this century [51]. The regional SSLA north of 40° N is near zero for 2005–2015, but it is dominated by changes in the Atlantic Ocean,

where the thermal and halosteric effects are opposite and largely cancel each other out. The Atlantic Ocean is characterized by density-compensating linear trends of TSLA and HSLA, at nearly all latitudes. A similar cancellation between TSLA and HSLA is also found in the North Indian Ocean. But in the the North Pacific Ocean (20° N–50° N), both TSLA and HSLA contribute to enhance SSLA. These complicated temperature and salinity changes highlight the complexity of ocean variability.

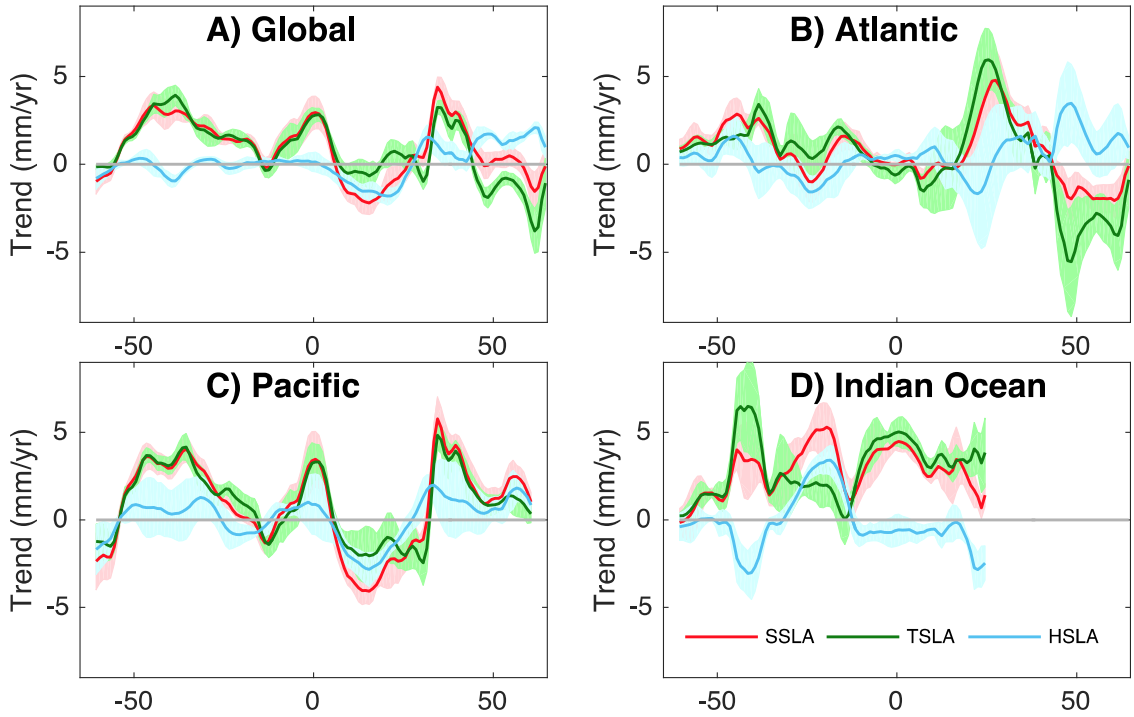

Figure 5. Zonal-averaged steric sea level trend in the global ocean (**A**); the Pacific Ocean (**B**); the Atlantic Ocean (**C**); and the Indian Ocean (**D**). Curves in different colors present the ensemble mean of SSLA (black), TSLA (red), and HSLA (blue), respectively. The standard deviation errors are attached in shadings.

In addition, we show the steric sea level changes in four main ocean basins in Table 2. The ocean basins are divided as Lee et al. (2015) [52], in which the Southern Ocean is directly connected to the Atlantic, Pacific, and Indian Oceans (at 35° S), and the other three basins are separated by their natural ocean-land boundaries. From a global perspective, the halosteric effect compensates the rapid steric sea level rise to some degree. The salinity-compensation effect mainly occurs in the Pacific Ocean and the Southern Ocean. While in the other two ocean basins, especially in the Indian Ocean, the halosteric effect enhances the steric sea level rise with thermal expansion together. The Pacific Ocean becomes saltier in basinal scale, and dominates the global mean HSLA, because of its large area (partially).

Table 2. Trend of SSLA, TSLA, and HSLA in the mainly ocean basins, unit: mm/yr. Values are ensemble means of all datasets and the two-time standard error.

	Atlantic	Indian	Pacific	Southern	Global
SSLA	0.77 ± 0.32	2.42 ± 0.45	0.0 ± 0.12	1.18 ± 0.25	0.80 ± 0.17
TSLA	0.74 ± 0.39	1.95 ± 0.37	0.22 ± 0.10	1.41 ± 0.28	0.85 ± 0.18
HSLA	0.04 ± 0.12	0.52 ± 0.10	-0.21 ± 0.05	-0.31 ± 0.12	-0.06 ± 0.03

A better illustration of the contribution of HSLA to SSLA can be obtained via an "explained variance" analysis. Here we use a fraction of variance (FOV) skill score to empirically quantify how much of the variance in SSLA can be explained by HSLA. FOV is calculated as:

$$FOV = \frac{cov(SSLA, HSLA)}{\sqrt{(cov(SSLA, HSLA))^2 + (cov(SSLA, TSLA))^2}} \quad (4)$$

where the covariance between SSLA and its independent processes are denoted as cov(SSLA, HSLA) and cov(SSLA, TSLA), respectively. According to this definition, a perfect score (FOV = 1) occurs when SSLA and HSLA are perfectly correlated with each other and have the same variance. If SSLA is only affected by the TSLA component, the FOV should be 0. Negative FOV indicates that HSLA is opposite to TSLA, so SSLA is the result of the competing temperature and salinity effects.

FOV in SSLA, explained by the halosteric component, is shown in Figure 6. The density compensating effect (FOV < 0) exists over a large portion of the global ocean, except in the north Pacific Ocean (35° N–60° N), the Subtropical Pacific Ocean (10° N–20° N), the Southern Ocean (40° S south), the Southeast Indian Ocean, and the western Tropical Atlantic Ocean. This is similar to our findings in Figure 5.

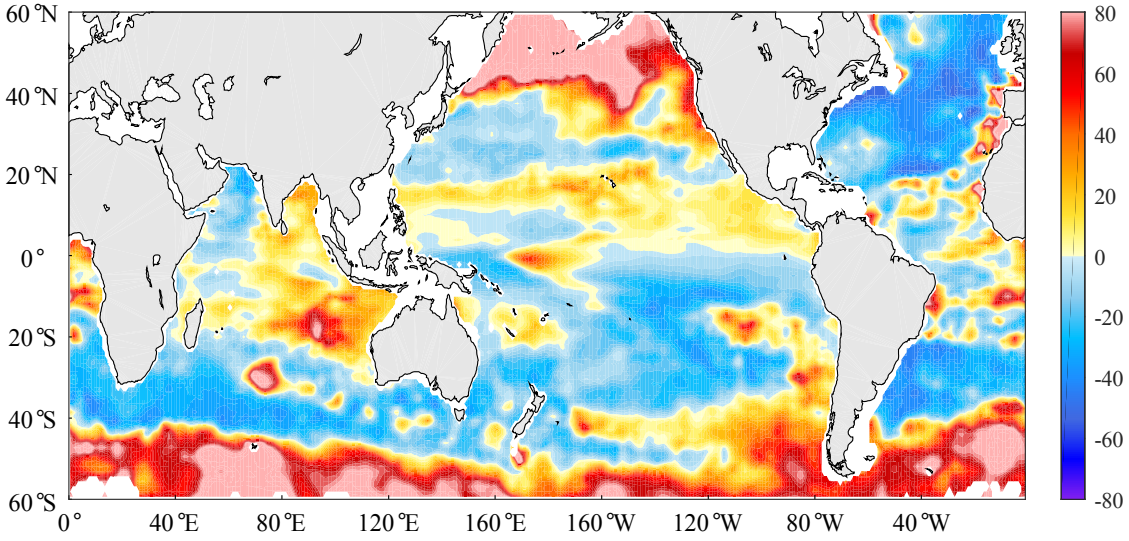

Figure 6. FOV of HSLA to the SSLA, during 2005 to 2015. Percentages (FOV X 100) shown here are used to illustrate the relative contribution of the halosteric component.

4. Summary and Conclusions

This study analyzed HSLA during the near-global Argo era (2005–2015), revisiting the role of the halosteric component in SSLA. The global mean (HSLA) experienced a decrease during 2005 to 2015, in contrast to the increase of TSLA. The trend of HSLA is -0.05 ± 0.03 mm/yr, which accounts for about -5.8% of SSLA (which ranges from 0 to 22% for different datasets), and partially offsets the strong thermal expansion (-5.6%, ranges from 0 to 18%). In addition, there is also interannual variability of HSLA, which is closely tied to ENSO.

Locally, the pattern of the HSLA trend shows negative trends in the subtropical ocean and positive trends in mid- and high latitudes. It is likely that this pattern is linked to the intensification of the global water cycle—the "wet gets wetter" scenario—under global warming [9]. Vertically, the ocean water became saltier in the upper 200-m layer and fresher in the 200 to 600-m layer, over 2005–2015. Below 600-m depth, the salinity trend is indistinguishable from zero. The HSLA trend is dominated by the salinity change in the upper 200-m layer, highlighting the importance of surface freshwater forcing.

The rich local salinity variability at different vertical layers highlights the role of salinity in our climate system. HSLA even dominates some regional SSLAs, for example, in the North Tropical Pacific Ocean and the Atlantic Ocean. Density compensation exists in almost all of the Atlantic Ocean, a portion of the Pacific (subtropical), and the Indian Ocean (mid-latitude region in the southern hemisphere). This implies we need to take account of both temperature and salinity to correctly represent density-driven circulation, such as the AMOC (Atlantic Meridional Overturning Circulation). In the Southern Ocean, both HSLA and TSLA components contribute to enhance SSLA.

This study is mostly based on data in the recent decade. The previous analyses, based on longer time series, show decadal variability [40]. Therefore, decadal and long-term salinity analyses still require more comprehensive studies in the future, once longer salinity time series are available. Since the underlying mechanisms of salinity changes are still not fully understood, it is urgent to examine the salinity change, via both reanalysis data and ocean models, and a simple budget analysis, such as [15–18] etc., is highly preferred to separate ocean dynamics with surface flux changes. It is also recommended to better reconstruct the historical ocean subsurface salinity field, given the importance of the halosteric sea level to the total sea level. This study provides a useful clue for the historical salinity reconstruction that the salinity changes are mostly confined at upper 600-m (or even 200-m, for the majority of the salinity changes).

Acknowledgments: We thank Jie Song and Jian Chen for discussions and two anonymous reviewers for helpful comments. L.C. is supported by the National Key R&D Program of China (2016YFC1401806 and 2016YFC1401705), 315030401. C.L. is supported by the National "973" Programme (No. 2013CB956203) and the National Natural Science Foundation of China (41490642). The data we used in this study are available in the Met Office of the UK for EN4 analysis (http://www.metoffice.gov.uk/hadobs/) and the Institute of Atmospheric Physics (CAS) for IAP dataset (http://159.226.119.60/cheng/). JAMSTEC data is available at ftp://ftp2.jamstec.go.jp/pub/argo/MOAA_GPV/Glb_PRS/OI/. SCRIPPS data is in http://sio-argo.ucsd.edu/RG_Climatology.html. NCEI data can be downloaded in https://www.nodc.noaa.gov/OC5/3M_HEAT_CONTENT/.

Author Contributions: G.W. and L.C. initiated this study, designed the experiments, and prepared figures and the first manuscript. T.B. and C.L. contributed to the design of the experiments and analysis of the results, and refined the manuscript.

Conflicts of Interest: The authors declare no conflict of interest. The funding sponsors had no role in the design of the study; in the collection, analysis, or interpretation of data; in the writing of the manuscript, and in the decision to publish the results.

References

1. Johnson, G.C.; Wijffels, S.E. Ocean Density Change Contributions to Sea Level Rise. *Oceanography* **2011**, *24*, 112–121. [CrossRef]
2. Antonov, J.I.; Levitus, S.; Boyer, T.P. Steric sea level variations during 1957–1994: Importance of salinity. *J. Geophys. Res. Oceans* **2002**, *107*, 8013. [CrossRef]
3. Willis, J.K.; Roemmich, D.; Cornuelle, B. Interannual variability in upper ocean heat content, temperature, and thermosteric expansion on global scales. *J. Geophys. Res. Oceans* **2004**, *109*, C12036. [CrossRef]
4. Lombard, A.; Cazenave, A.; Letraon, P.; Ishii, M. Contribution of thermal expansion to present-day sea-level change revisited. *Glob. Planet. Chang.* **2005**, *47*, 1–16. [CrossRef]
5. Levitus, S.; Antonov, J.I.; Boyer, T.P.; Baranova, O.K.; Garcia, H.E.; Locarnini, R.A.; Mishonov, A.V.; Reagan, J.R.; Seidov, D.; Yarosh, E.S.; et al. World ocean heat content and thermosteric sea level change (0–2000 m), 1955–2010. *Geophys. Res. Lett.* **2012**, *39*, L10603–L10607. [CrossRef]
6. Church, J.A.; White, N.J.; Konikow, L.F.; Domingues, C.M.; Cogley, J.G.; Rignot, E.; Gregory, J.M.; van den Broeke, M.R.; Monaghan, A.J.; Velicogna, I. Revisiting the Earth's sea-level and energy budgets from 1961 to 2008. *Geophys. Res. Lett.* **2011**, *38*, L18601. [CrossRef]
7. Llovel, W.; Willis, J.K.; Landerer, F.W.; Fukumori, I. Deep-ocean contribution to sea level and energy budget not detectable over the past decade. *Nat. Clim. Chang.* **2014**, *4*, 1031–1035. [CrossRef]
8. Boyer, T.P.; Antonov, J.I.; Baranova, O.K.; Coleman, C.; Garcia, H.E.; Grodsky, A.; Johnson, D.R.; Locarnini, R.; Mishonov, A.; O'Brien, T.D.; et al. *World Ocean Database 2013*; NOAA Atlas NESDIS: Silver Spring, MD, USA, 2013.

9. Durack, P.J.; Wijffels, S.A.; Gleckler, P.J. Long-term Sea-level Change Revisited: The Role of Salinity. *Environ. Res. Lett.* **2014**, *9*, 114017. [CrossRef]
10. Maes, C. Estimating the influence of salinity on sea level anomaly in the ocean. *Geophys. Res. Lett.* **1998**, *25*, 3551–3554. [CrossRef]
11. Levitus, S.; Antonov, J.I.; Boyer, T.P.; Garcia, H.E.; Locarnini, R.A. Linear trends of zonally averaged thermosteric, halosteric, and total steric sea level for individual ocean basins and the world ocean, (1955–1959)–(1994–1998). *Geophys. Res. Lett.* **2005**, *32*. [CrossRef]
12. Suzuki, T.; Ishii, M. Long-term regional sea level changes due to variations in water mass density during the period 1981–2007. *Geophys. Res. Lett.* **2011**, *38*, L21604. [CrossRef]
13. Sato, O.T.; Polito, P.S.; Liu, W.T. Importance of salinity measurements in the heat storage estimation from TOPEX/POSEIDON. *Geophys. Res. Lett.* **2000**, *27*, 549–551. [CrossRef]
14. Wunsch, C.; Rui, M.P.; Heimbach, P. Decadal Trends in Sea Level Patterns: 1993–2004. *J. Clim.* **2007**, *20*, 5889–5911. [CrossRef]
15. Yu, L. A global relationship between the ocean water cycle and near-surface salinity. *J. Geophys. Res.* **2011**, *116*, C10025. [CrossRef]
16. Hasson, A.E.A.; Delcroix, T.; Dussin, R. An assessment of the mixed layer salinity budget in the tropical Pacific Ocean. Observations and modelling (1990–2009). *Ocean Dyn.* **2013**, *63*, 179–194. [CrossRef]
17. Du, Y.; Zhang, Y.; Feng, M.; Wang, T.; Zhang, N.; Wijffels, S. Decadal trends of the upper ocean salinity in the tropical Indo-Pacific since mid-1990s. *Sci. Rep.* **2015**, *5*, 16050. [CrossRef] [PubMed]
18. Ponte, R.M.; Vinogradova, N.T. An assessment of basic processes controlling mean surface salinity over the global ocean. *Geophys. Res. Lett.* **2016**, *43*, 7052–7058. [CrossRef]
19. Durack, P.J.; Wijffels, S.E. Fifty-Year Trends in Global Ocean Salinities and Their Relationship to Broad-Scale Warming. *J. Clim.* **2010**, *23*, 4342–4362. [CrossRef]
20. Skliris, N.; Marsh, R.; Josey, S.A.; Good, S.A.; Liu, C.; Allan, R.P. Salinity changes in the World Ocean since 1950 in relation to changing surface freshwater fluxes. *Clim. Dyn.* **2014**, *43*, 709–736. [CrossRef]
21. Hosoda, S.; Suga, T.; Shikama, N.; Mizuno, K. Global surface layer salinity change detected by Argo and its implication for hydrological cycle intensification. *J. Oceanogr.* **2009**, *65*, 579–586. [CrossRef]
22. Durack, P.J.; Wijffels, S.E.; Matear, R.J. Ocean salinities reveal strong global water cycle intensification during 1950 to 2000. *Science* **2012**, *336*, 455–458. [CrossRef] [PubMed]
23. Zhang, L.; Wu, L. Can Oceanic Freshwater Flux Amplify Global Warming? *J. Clim.* **2012**, *25*, 3417–3430. [CrossRef]
24. Levitus, S. Interpentadal variability of steric sea level and geopotential thickness of the north Atlantic Ocean, 1970–1974 versus 1955–1959. *J. Geophys. Res. Atmos.* **1990**, *95*, 5233–5238. [CrossRef]
25. Ishii, M.; Kimoto, M.; Sakamoto, K.; Iwasaki, S.-I. Steric Sea Level Changes Estimated from Historical Ocean Subsurface Temperature and Salinity Analyses. *J. Oceanogr.* **2006**, *62*, 155–170. [CrossRef]
26. Talley, L.D.; Pickard, G.L.; Emery, W.J. (Eds.) *Descriptive Physical Oceanography: An Introduction*, 6th ed.; Academic Press: Amsterdam, The Netherlands; Boston, MA, USA, 2011.
27. Fasullo, J.T.; Boening, C.; Landerer, F.W.; Nerem, R.S. Australia's unique influence on global sea level in 2010–2011. *Geophys. Res. Lett.* **2013**, *40*, 4368–4373. [CrossRef]
28. Fasullo, J.; Nerem, R. Interannual Variability in Global Mean Sea Level Estimated from the CESM Large and Last Millennium Ensembles. *Water* **2016**, *8*, 491. [CrossRef]
29. Llovel, W.; Lee, T. Importance and origin of halosteric contribution to sea level change in the southeast Indian Ocean during 2005–2013. *Geophys. Res. Lett.* **2015**, *42*, 1148–1157. [CrossRef]
30. Cheng, L.; Trenberth, K.E.; Fasullo, J.; Boyer, T.; Abraham, J.; Zhu, J. Improved estimates of ocean heat content from 1960 to 2015. *Sci. Adv.* **2017**, *3*, e1601545. [CrossRef] [PubMed]
31. Cheng, L.; Zhu, J. Benefits of CMIP5 multimodel ensemble in reconstructing historical ocean subsurface temperature variations. *J. Clim.* **2016**, *29*, 5393–5416. [CrossRef]
32. Barnes, S.L. A technique for maximizing details in numerical weather map analysis. *J. Appl. Meteorol.* **1964**, *3*, 396–409. [CrossRef]
33. Jayne, S.R.; Wahr, J.M.; Bryan, F.O. Observing ocean heat content using satellite gravity and altimetry. *J. Geophys. Res. Atmos.* **2003**, *108*, 295–314. [CrossRef]
34. McDougall, T.J. Neutral Surface. *J. Phys. Oceanogr.* **1987**, *17*, 1950–1964. [CrossRef]

35. Cazenave, A.; Dieng, H.-B.; Meyssignac, B.; von Schuckmann, K.; Decharme, B.; Berthier, E. The rate of sea-level rise. *Nat. Clim. Chang.* **2014**, *4*, 358–361. [CrossRef]
36. Wilks, D.S. *Statistical Methods in the Atmospheric Sciences*; Academic Press: Oxford, UK, 2011; Volume 100.
37. Yu, L.; Jin, X.; Josey, S.A.; Lee, T.; Kumar, A.; Wen, C.; Xue, Y. The Global Ocean Water Cycle in Atmospheric Reanalysis, Satellite, and Ocean Salinity. *J. Clim.* **2017**, *30*, 3829–3852. [CrossRef]
38. Purkey, S.G.; Johnson, G.C. Antarctic Bottom Water Warming and Freshening: Contributions to Sea Level Rise, Ocean Freshwater Budgets, and Global Heat Gain. *J. Clim.* **2013**, *26*, 6105–6122. [CrossRef]
39. Menezes, V.V.; Macdonald, A.M.; Schatzman, C. Accelerated freshening of Antarctic Bottom Water over the last decade in the Southern Indian Ocean. *Sci. Adv.* **2017**, *3*, e1601426. [CrossRef] [PubMed]
40. Boyer, T.; Levitus, S.; Antonov, J.; Locarnini, R.; Mishonov, A.; Garcia, H.; Josey, S.A. Changes in freshwater content in the North Atlantic Ocean 1955–2006. *Geophys. Res. Lett.* **2007**, *34*, 159–166. [CrossRef]
41. Cazenave, A.; Henry, O.; Munier, S.; Delcroix, T.; Gordon, A.L.; Meyssignac, B.; Llovel, W.; Palanisamy, H.; Becker, M. Estimating ENSO Influence on the Global Mean Sea Level, 1993–2010. *Mar. Geod.* **2012**, *35*, 82–97. [CrossRef]
42. Stammer, D.; Cazenave, A.; Ponte, R.M.; Tamisiea, M.E. Causes for Contemporary Regional Sea Level Changes. *Annu. Rev. Mar. Sci.* **2013**, *5*, 21–46. [CrossRef] [PubMed]
43. Lago, V.; Wijffels, S.E.; Durack, P.J.; Church, J.A.; Bindoff, N.L.; Marsland, S.J. Simulating the role of surface forcing on observed multidecadal upper ocean salinity changes. *J. Clim.* **2015**, *29*, 5575–5588. [CrossRef]
44. Llovel, W.; Meyssignac, B.; Cazenave, A. Steric sea level variations over 2004–2010 as a function of region and depth: Inference on the mass component variability in the North Atlantic Ocean. *Geophys. Res. Lett.* **2011**, *38*, 601–612. [CrossRef]
45. Curry, R.G.; McCartney, M.S.; Joyce, T.M. Oceanic transport of subpolar climate signals to mid-depth subtropical waters. *Nature* **1998**, *391*, 575–577. [CrossRef]
46. Köhl, A.; Sena Martins, M.; Stammer, D. Impact of assimilating surface salinity from SMOS on ocean circulation estimates. *J. Geophys. Res. Oceans* **2014**, *119*, 5449–5464. [CrossRef]
47. Lu, Z.; Cheng, L.; Zhu, J.; Lin, R. The complementary role of SMOS sea surface salinity observations for estimating global ocean salinity state. *J. Geophys. Res. Oceans* **2016**, *121*, 3672–3691. [CrossRef]
48. Wijffels, S.; Roemmich, D.; Monselesan, D.; Church, J.; Gilson, J. Ocean temperatures chronicle the ongoing warming of Earth. *Nat. Clim. Chang.* **2016**, *6*, 116–118. [CrossRef]
49. Llovel, W.; Terray, L. Observed southern upper-ocean warming over 2005? 2014 and associated mechanisms. *Environ. Res. Lett.* **2016**, *11*, 124023. [CrossRef]
50. Volkov, D.L.; Lee, S.-K.; Landerer, F.W.; Lumpkin, R. Decade-long deep-ocean warming detected in the subtropical South Pacific: Deep-Ocean Warming in the South Pacific. *Geophys. Res. Lett.* **2017**, *44*, 927–936. [CrossRef]
51. Hu, S.; Sprintall, J. Observed strengthening of interbasin exchange via the Indonesian seas due to rainfall intensification. *Geophys. Res. Lett.* **2017**, *44*, 1448–1456. [CrossRef] [PubMed]
52. Lee, S.-K.; Park, W.; Baringer, M.O.; Gordon, A.L.; Huber, B.; Liu, Y. Pacific origin of the abrupt increase in Indian Ocean heat content during the warming hiatus. *Nat. Geosci.* **2015**, *8*, 445–449. [CrossRef]

© 2017 by the authors. Licensee MDPI, Basel, Switzerland. This article is an open access article distributed under the terms and conditions of the Creative Commons Attribution (CC BY) license (http://creativecommons.org/licenses/by/4.0/).